Scaling in Turbulence

Data Science Computer Lab Project 1

András Mátyás Biricz
Benedek Horváth

October 26 2018

Contents

1 Introduction

Dissipation rate and enstrophy have been observables of great interest in turbulence research due to their dynamical significance for the evolution of flow and their rich spatial structure and intermittent nature. In a view dating back to Kolmogorov and Obukhov, the transfer of kinetic energy from large to small scales proceeds as a self-similar cascade process. The presence of power-laws in the velocity spectrum, velocity structure functions and moments of velocity gradients and dissipation are seen as an indication of such self-similar behaviour [1]. Our aim is to study the power-law scaling property of forced isotropic turbulent flow.

2 Definitions

In the study of turbulence, there are some relevant scalar fields derived from the velocity gradient tensor ($\nabla \mathbf{u}$). Here we consider the so-called **enstrophy**,

$$\frac{1}{2}\omega^2(\mathbf{x}) = \frac{1}{2}(\nabla \times \mathbf{u})^2 = \frac{1}{2}\epsilon_{ijk}\epsilon_{klm}\partial_i u_j \partial_l u_m, \tag{1}$$

and **dissipation**,

$$S^2(\mathbf{x}) = S_{ij}S_{ij}, \text{ where} \tag{2}$$

$$S_{ij} = \frac{1}{2}(\nabla \mathbf{u} + \nabla \mathbf{u}^T)_{ij} = \frac{1}{2}(\partial_i u_j + \partial_j u_i). \tag{3}$$

In this study we examine certain sets of points. The **indicator function** of a set is defined as

$$\Theta_\chi(\mathbf{x}) = \begin{cases} 1, & \text{if } \mathbf{x} \in \text{set of interest associated with threshold } \chi \\ 0, & \text{otherwise.} \end{cases} \tag{4}$$

The idea of excursion set means a set of points where a certain observable is above a certain limit. The motivation behind this concept is to be able to analyze only the most important flow-field regimes. The so-called indicator function of an excursion set of a scalar field $A(x)$, for a threshold χ:

$$\Theta^A_\chi(\mathbf{x}) = H(A(\mathbf{x}) - \chi) = \begin{cases} 1, & \text{if } A(\mathbf{x}) \geq \chi \\ 0, & \text{otherwise.} \end{cases} \tag{5}$$

For example, the excursion set for the enstrophy (denoted by E here) for the threshold $\chi = 20\langle S^2 \rangle$:

$$E_\chi(\mathbf{x}) = E(\mathbf{x})\Theta^E_\chi(\mathbf{x}) = E(\mathbf{x})\Theta^E_{20\langle S^2\rangle}(\mathbf{x}) = \begin{cases} E(\mathbf{x}), & \text{if } E(\mathbf{x}) \geq 20\langle S^2 \rangle \\ 0, & \text{otherwise.} \end{cases} \tag{6}$$

In this work all threshold values used are multiples of the space-average dissipation, $\langle S^2 \rangle$. We will examine enstrophy and dissipation excursion sets, however, defining the thresholds as multiples of $\langle S^2 \rangle$ is correct, since the space-averages of enstrophy and dissipation are equal in isotropic turbulence.

The self-similarity of a turbulent flow can be demonstrated by examining the correlation function of the indicator function of a given excursion set. The two-point correlation is:

$$\mathcal{C}_\chi(\mathbf{r}) = \langle \Theta_\chi(\mathbf{x}) \Theta_\chi(\mathbf{x}+\mathbf{r}) \rangle, \tag{7}$$

where the average means spatial average over positions $\mathbf{x}$. From here on, the angular average of the 3-dimensional correlation function can be calculated, which depends only on the absolute value of the distance r from the origin:

$$\mathcal{C}_\chi(r) = \frac{1}{\mathcal{C}_\chi(\mathbf{0})} \int \mathcal{C}_\chi(\mathbf{r}) d\Omega_{\mathbf{r}}. \tag{8}$$

One can expect that the correlation function decays according to a power-law:

$$\mathcal{C}_\chi(r) \propto K_\chi r^{-\gamma_\chi}, \tag{9}$$

where the parameters obviously depend on the threshold. According to the theory of fractals (i.e. self-similar objects) one can say that

$$\mathcal{C}_\chi(r) \propto r^{D-E}, \tag{10}$$

where D is the so-called correlation dimension and E is the dimension of the embedding space, which is 3 in this case. Thus the value of the correlation dimension is:

$$D(\chi) = 3 - \gamma_\chi. \tag{11}$$

In a 3-dimensional forced turbulent flow the energy is injected into the system at a specific length-scale. Since the energy of the flow can be decreased by friction only by transforming it into heat, it is dissipated at the scale where this process dominates, i.e. at the so-called Kolmogorov-scale, denoted by η. In between lies the inertial range where the direct energy cascade can be observed. According to the predictions of Kolmogorov:

$$E(k) \propto k^{-\frac{5}{3}}. \tag{12}$$

3 Dataset and Methods

To investigate the scaling behaviour of turbulence we use already existing simulation data. In the Johns Hopkins Turbulent Database direct numerical simulation (DNS) of various kind of turbulent flows are accessible. Here we restrict ourselves to the case of isotropic turbulence as the study in [1].

The simulation data of the forced isotropic turbulent flow has the following properties:

- 1024 nodes in each direction.
- Energy is injected by keeping constant the total energy in shells such that $|k|$ is less or equal to 2.
- After the simulation has reached a statistical stationary state, 5028 frames of data with 3 velocity components and pressure are stored in the database. Extra time frames at the beginning and at the end are available to be used for temporal-interpolations.
- The Taylor-scale Reynolds number fluctuates around $R_\lambda \approx 433$.

More information can be found on the webpage of the database[1]. To access the data in the database one needs to have an authorization token. This can be acquired simply via e-mail message to an address given on the webpage[2]. In the present study the simulation data is downloaded at the time frame $t = 0.0$ s.

As the number of computational grid points is in the 10^9 order of magnitude, the data for the grid are in the gigabyte range. The maximum size of sub-grid that was possible to be downloaded in one request to the database server was 128^3. Thus, we had to run multiple requests for different cubes of the whole grid and merging the data into one file. We made a 256^3 and a 512^3 data file via 8 and 64 requests, respectively. Both of them contains the cube $[0,\ L]^3$ near the origin. In addition, we also made a data file 256^3 by extracting every 4^{th} element of the original 1024^3 grid in each direction. Note that the size of the data file that contains the coordinates, velocities and velocity gradients for the 512^3 cube is 21 GB, while running the Jupyter Notebook for our data analysis the memory consumption was nearly 40 GB memory.

Working with the data of the isotropic turbulent flow, it is wise to recall the major properties of the pseudo-spectral DNS simulation. It assumes, that the simulation domain is periodic in each direction, the boundary conditions are periodic and the unknown quantity (e.g. velocity) should be also a periodic function.

$$\frac{\partial \mathbf{u}}{\partial t} - \mathbf{u} \times \omega = \nu \nabla^2 \mathbf{u} - \nabla P, \tag{13}$$

$$\nabla \cdot \mathbf{u} = 0, \tag{14}$$

$$\mathbf{u}(\mathbf{x} + 2\pi \mathbf{e}^{(i)}, t) = \mathbf{u}(\mathbf{x}, t); \quad i = 1, 2, 3, \tag{15}$$

where $\mathbf{u}(\mathbf{x}, t)$ is the velocity field, $\omega = \nabla \times \mathbf{u}$ is the vorticity, $\mathbf{e}^{(i)}$ are the basis vectors of the Cartesian coordinate system, $P = \frac{p}{\rho} + \frac{\mathbf{u} \cdot \mathbf{u}}{2}$ is the modified pressure, where p denotes the normal pressure quantity. Since the velocity field is periodic, the following equations describe the transformations between the real and Fourier-spaces:

[1] http://turbulence.pha.jhu.edu/Forced_isotropic_turbulence.aspx
[2] http://turbulence.pha.jhu.edu/authtoken.aspx

$$u(\mathbf{x},t) = \frac{1}{N_x N_y N_z} \sum_{\mathbf{k}} \hat{u}_k(t) e^{i\mathbf{kx}}, \tag{16}$$

$$\hat{u}_k = \sum_{\mathbf{x}} u(\mathbf{x},t) e^{-i\mathbf{kx}}, \tag{17}$$

where $\hat{u}_k(t)$ denotes the Fourier-components, i is the imaginary unit, $e^{i\mathbf{kx}}$ are the basis functions of the presented method.

The major advantage of this numerical method is to convert the system of partial differential equations into one ordinary differential equation that can be solved by for example a 4^{th} order Runge-Kutta method. It is achieved by transforming the above presented equations (13, 14) and expressing the pressure. As a result one may get:

$$\frac{d\hat{\mathbf{u}}_k}{dt} = (\mathbf{u} \hat{\times} \omega)_k - \nu|\mathbf{k}|^2 \hat{\mathbf{u}}_k - \mathbf{k}\frac{\mathbf{k} \cdot (\mathbf{u} \hat{\times} \omega)_k}{|\mathbf{k}|^2}, \tag{18}$$

where the cross products are transformed to Fourier-space after calculated in real space.

More details about this method can be found in the literature or in [2].

4 Results and discussion

4.1 Comparision of two schemes of numerical differentiation

Figure 1 illustrates the $\frac{\partial v_x}{\partial x}$ component of the velocity gradient obtained by the spectral differentiation and the 4^{th}-order finite difference scheme. For comparison both are plotted on the same graph at a slice in the x direction. We checked the velocity gradient for two different cases: we calculated it (i) on the $[0,\ 256]^3$ continuous box of the 1024^3 grid and (ii) on a 256^3 box gained by extracting every 4^{th} element of the original grid in each direction. In the left panel of the plot, which shows the gradient for the continuous box, it can be seen that an artificial noise appears (see the region near $x = 0$). The reason is that this dataset does not contain the whole periodic domain, which results in an artifact when the spectral differentiation method is used. However, the finite difference method works everywhere and returns fairly good results. The right panel belongs to the coarse dataset, in which only every fourth grid points were taken into account in each dimension. In this case the results calculated via the two different methods show a good agreement, because the range of the coordinates is $[0,\ 2\pi]$, i.e. it is periodic. However, the results are different from that one obtained for the continuous box, since the spatial resolution of the grid is significantly lower. One more point is that the most important region of the correlation function is the one for low distances. In order to obtain correct results for the correlation function, it is essential to use a continuous dataset in our further analyses. As a conclusion, we decided to use the continuous 512^3 dataset and calculate the velocity gradient via 4^{th}-order finite difference scheme in the further calculations.

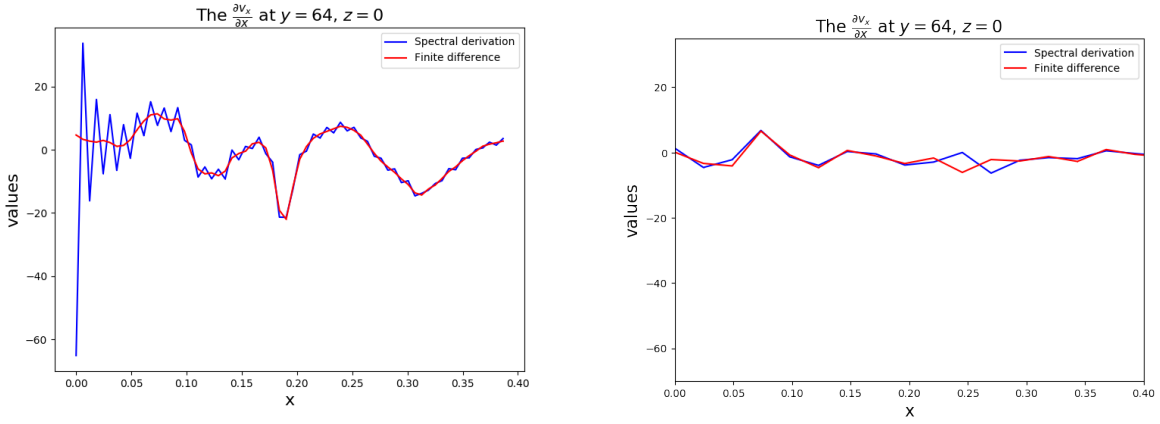

Figure 1: Comparison of the spectral derivation and finite difference methods for calculating the velocity gradient. *Left:* calculated on the $[0, 256]^3$ continuous box of the 1024^3 grid. *Right:* calculated on a 256^3 box gained by extracting every 4^{th} element of the original grid in each direction.

4.2 Excursion set analysis

Given a threshold the indicator function can be calculated and its full two-point correlation can be given via convolution. In practice, this can be determined in Fourier-space with multiplications and then transformed back to real space. At this point the correlation values are given everywhere in the simulation domain, so those are direction dependent. Since we are interested in only the distance dependence, the angular average of the correlation function should be given at each radius. The data cube obviously represents the points in Cartesian coordinates. To be able to resolve the angular averaging we assigned spherical coordinates to each point. From the list of points obtained we sorted out the different radii and performed integration on each of the surfaces. As a result we got the correlation function that depends purely on the radial coordinate. For scaling arguments it is wise to scale the radius values in Kolmogorov-length.

Figure 2 shows the power-law decaying behaviour of the correlation function of enstrophy and dissipation excursion sets for threshold values ranging from 7 to 50 times the spatial average of dissipation. The fitted exponents and correlation dimensions are shown on the subfigures. Note that the power-law behaviour is only true in the inertial range, which is between the energy injection scale and the dissipation (Kolmogorov) scale. According to this argument only a sub-interval is selected for fitting.

The graphs explain that if the threshold is smaller the correlation is stronger. This is true for enstrophy and dissipation excursion sets as well. Simple explanation can be that there are more "interesting points" marked by the indicator function in the flow-field if we choose smaller threshold values. The rightmost graph at the bottom shows that if the threshold is sufficiently high a scaling correlation function is still observable, but with large errors.

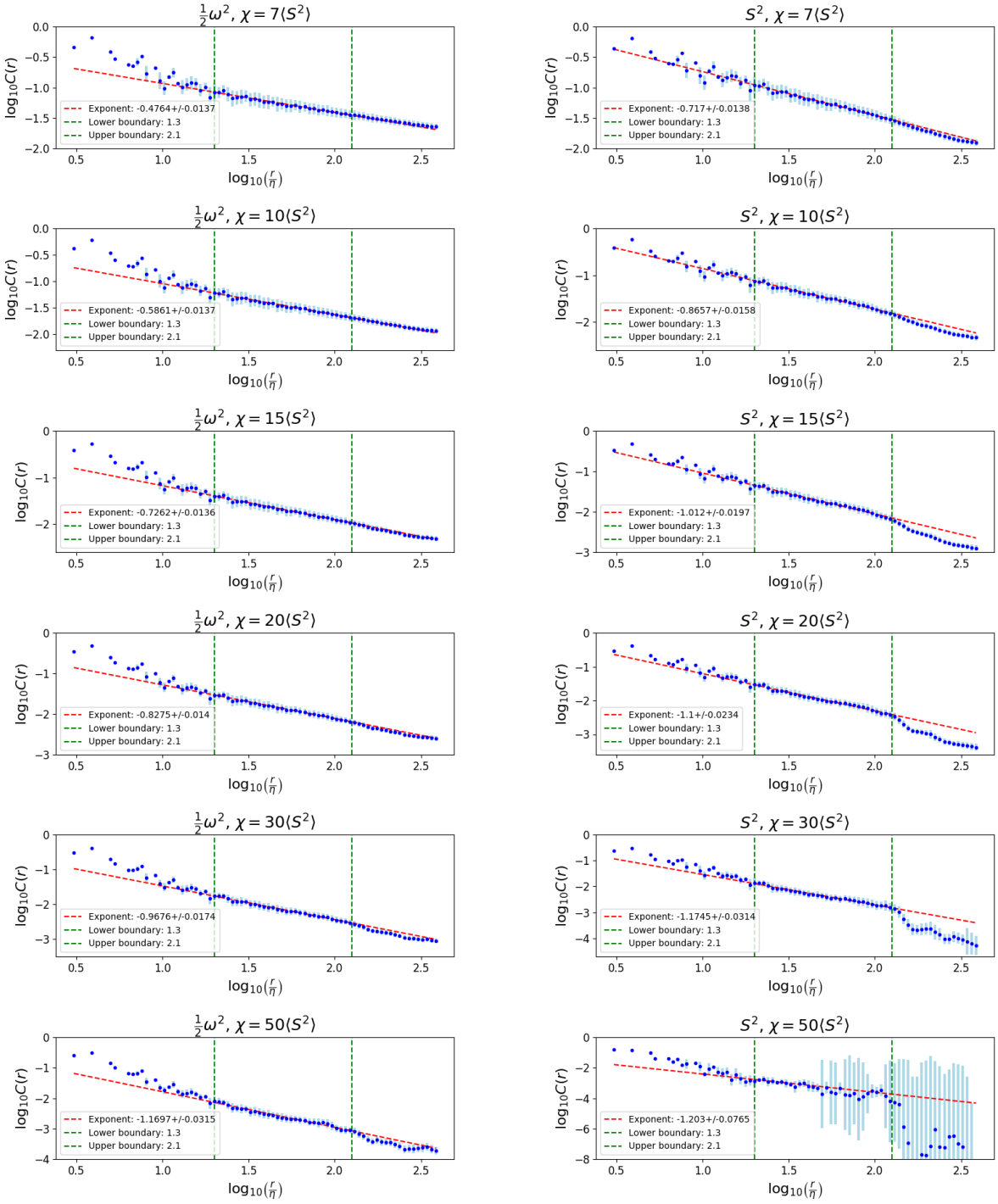

Figure 2: Correlation as a function of distance measured on Kolmogorov length scale, for the excursion sets of enstrophy (*left side*) and dissipation (*right side*), for various threshold values.

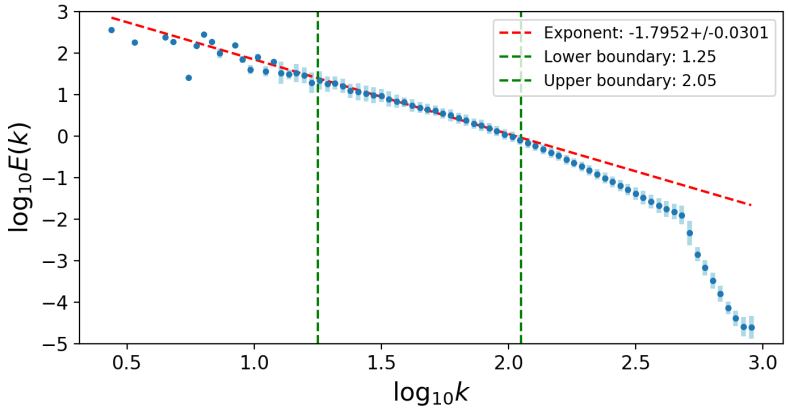

Figure 3: The spatial energy spectrum as a function of the absolute value of the wavenumber, calculated on the $[0, 512]^3$ continuous box of the 1024^3 grid. The forward energy-cascade exponent is fitted in the inertial range.

The errors are calculated after the angular average process is performed by integration. The simulation domain is a box originally, but it is converted into shells at all possible radius values. At higher radius values there are much more shells in a certain small interval than at lower radius values, thus the number density of computed values will be much larger at larger scales. (It can be shown by calculating a histogram of the radius values.) After defining a fixed resolution for the whole domain (fixing the number of bins) averages and deviations can be calculated in each small interval for the values of the correlation function. This is the way how the errors are calculated and taken into account in the linear fit.

4.3 Energy spectrum

Figure 3 shows the spatial energy spectrum calculated on the domain $[0, 512]^3$. The errors here are computed the same way as for the correlation function before. The spectrum gives information about the kinetic energy density in various spatial structures, i.e. vortices. Investigating this graph it can be found that there should exist self-similar structures for at least over one order of magnitude. The dimension of this fractal behaviour is almost the same as predicted by Kolmogorov (equation 12). At large wavenumber (k) values the kinetic energy can dissipate from the system, therefore a cutoff is expected.

5 Conclusions

Our aim was to show the scaling properties and fractal behaviour of turbulent flow. The indicator function and its correlation were determined and scaling in case of enstrophy and dissipation excursion sets were proved. In addition, the 3-dimensional spatial spectrum was calculated and its direct dependence on the absolute value of k was given. Despite we could only use a sub-domain (512^3 grid points instead of 1024^3), the results are close to what is presented in [1]. If there had been more computational resources available, calculations on the whole simulation domain could have been carried out providing more accurate results.

References

[1] J. H. Elsas, A. S. Szalay, and C. Meneveau, "Geometry and Scaling Laws of Excursion and Iso-sets of Enstrophy and Dissipation in Isotropic Turbulence," aug 2017. [Online]. Available: http://arxiv.org/abs/1708.05409http://dx.doi.org/10.1080/14685248.2018.1424995

[2] M. Mortensen and H. P. Langtangen, "High performance Python for direct numerical simulations of turbulent flows," *Computer Physics Communications*, vol. 203, pp. 53–65, jun 2016. [Online]. Available: https://www.sciencedirect.com/science/article/pii/S0010465516300200?via{%}3Dihub